

PSI INJECTOR II AND THE 72 MeV TRANSFER LINE: MinT-SIMULATION vs. MEASUREMENTS

C. Baumgarten*, H. Zhang, Paul Scherrer Institut, 5232 Villigen PSI, Switzerland

Abstract

PSI's Injector II cyclotron is the only cyclotron worldwide that makes use of the so-called "Vortex effect", in which the space charge force leads to the counter-intuitive effect to "roll up" bunches, thus keeping them longitudinally compact. The effect has been confirmed by bunch shape measurements and the PIC-simulations with OPAL. However, PSI's new fast matrix code MinT allows to reproduce the Vortex effect by a linear matrix model which is computational much cheaper than PIC simulations, and is suitable for "online use" in Control rooms. Furthermore it provides the second moments σ_{ij} of matched distributions.

We compare results of various measurements with MinT calculations which show that the linear model works well and provides excellent initial conditions to fit the beam profiles of the 72 MeV transfer line to the Ring cyclotron.

INTRODUCTION

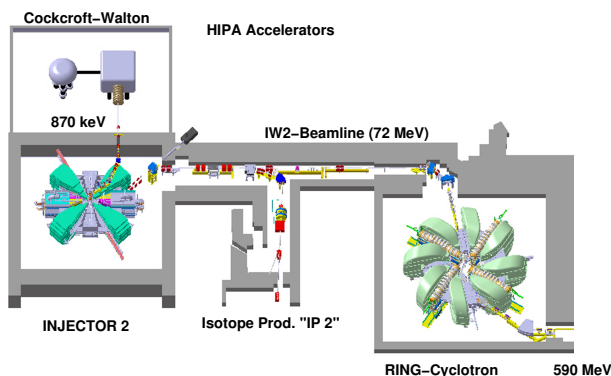


Figure 1: Accelerator part of PSI's high intensity accelerator facility (HIPA).

Figure 1 shows PSI's High Intensity Proton Accelerator (HIPA): A Cockcroft-Walton DC pre-accelerator provides a 870 keV proton beam of typically 10 mA DC current. Two (first and third harmonic) bunches are used to generate 50 MHz CW bunch structure before the beam is axially injected into the first turn of Injector II as shown in Fig. 2. Due to the Vortex effect the bunches remain almost round. The beam is extracted at 72 MeV from Injector II and transported with the IW2-beamline towards the PSI's Ring cyclotron. The 590 MeV beam is used to generate pions and muons at two graphite targets and for neutron production in the Swiss spallation source SINQ [1].

* christian.baumgarten@psi.ch

THE VORTEX EFFECT

The Vortex effect [2] (or "negative mass instability" [3]) is due to strong space charge of bunches in the isochronous regime of circular accelerators. The space charge force induces coupling terms between the longitudinal and the transverse-horizontal beam motion [4, 5]. This coupling leads to a dense and matched core bunch and (typically) a halo with two tails [6, 7]. In the bunch core the space charge force is approximately linear and the linear matching conditions can be computed, if beam current and core emittances are known [5, 8]. The halo tails of the bunches

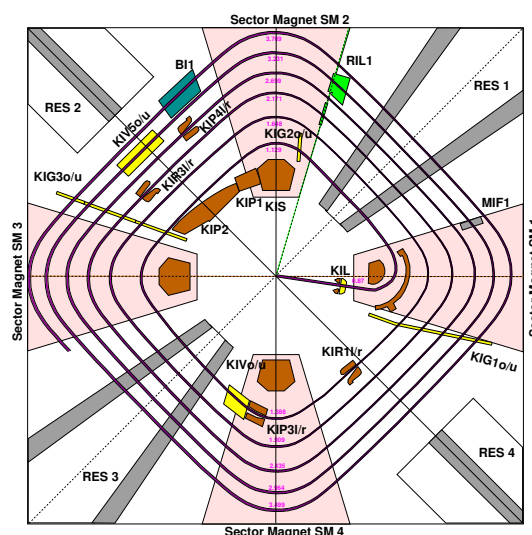


Figure 2: Central region of the Injector II cyclotron. Several movable collimators (KIP3, KIR1, KIP4) allow to remove halo in support of a clean bunch formation. The first few turns of the beam path are shown as well.

are cleaned by horizontal collimators if the orientation of the tails is transverse. However, the orientation of the halo tails depends on the details of the bunch formation and the strength of the space charge force, i.e. the beam current. As shown in Fig. 2, the first turns of Injector II are equipped with several sets of movable collimators. The radial position of the "KIP2" collimator is used to control the beam current. The other collimators allow for a setup with low losses at extraction.

However, if the orientation of the halo tails depends on the beam current, then the extraction losses caused by the halo tails will also depend on the bunch charge. Figure 3 shows the losses of the ionization chamber "MII6" located at the extraction of Injector II versus beam current, measured with current monitor "MXC1". The losses show a strongly non-linear, almost periodic, dependency on the current. In case of a strong Vortex effect, one expects that filamentation

Content from this work may be used under the terms of the CC-BY-4.0 licence (© 2023). Any distribution of this work must maintain attribution to the author(s), title of the work, publisher, and DOI

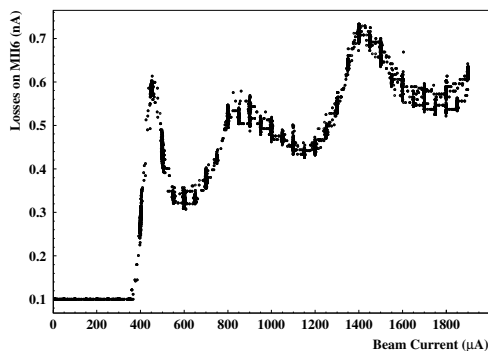


Figure 3: Extraction losses vs. beam current, measured with ionization chamber “MII6” located behind the electrostatic extractor “EID” of the Injector II cyclotron.

of the beam leads to a self-matching of the core bunch, while the beam halo will either be removed by collimators and/or will lead to increased losses at extraction. The effectiveness of the collimators depends on the orientation of the halo tails, which in general depends on the bunch charge as illustrated in Fig. 4.

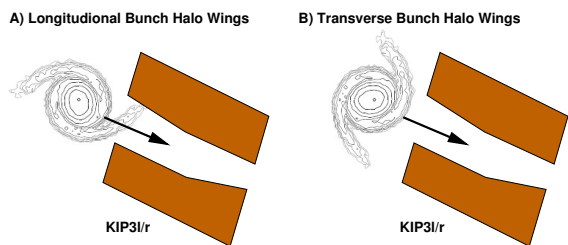


Figure 4: The effect of horizontal collimators depends on the orientation of the halo tails relative to the collimator aperture.

THE IW2 BEAMLINE

A simulation of the 72 MeV (“IW2”) transfer beamline with the PIC-code OPAL [9] with space charge has been presented in Ref. [10]. But the use of PIC-codes is computational expensive. An alternative is the use of a linearized approximation [5] which allows to model the Vortex effect by TRANSPORT type matrix methods. This has been implemented in PSI’s new fast and linear beam code MinT (MinT is not Transport) [11]. A sequence of symplectic transformations allows to compute the matched beam parameters in isochronous machines for given current and emittance(s) [5, 12].

As shown in Fig. 5, the matched beam in the last turn of Injector II, provides excellent starting conditions for beam optics computation of the IW2 beamline. The only free parameters for the fit of the horizontal beam envelope are the horizontal (longitudinal) emittance $\varepsilon = \varepsilon_x \equiv \varepsilon_z$. In a first step (dark colors), all beam profiles, horizontal and vertical are fitted by two parameters, the vertical and the transverse emittances. The vertical phase space distribution is not

necessarily matched, and the fit could be (slightly) improved in a second step by varying the three vertical parameters σ_{33} , σ_{34} , σ_{44} . The resulting envelopes are shown in brighter colors.

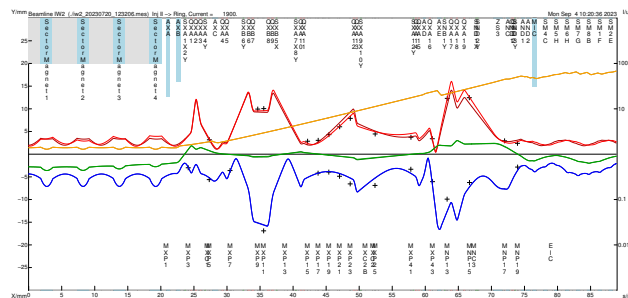


Figure 5: MinT beam optics calculation of the IW2 beamline at a beam current of 1.9 mA, assuming a fully matched beam (dark colors) and - in light colors - a horizontally matched beam with the vertical beam parameters matched to reproduce the measured beam sizes (cross markers). The dispersion (green), the vertical ($2\sigma_y$, red), the horizontal ($-2\sigma_x$, blue) and the longitudinal beam size ($\sigma_z/2$, orange) are indicated by solid lines.

BEAM EMITTANCE VS. CURRENT

The beam profiles in IW2 were measured at various beam currents. Fits of the ion optics using MinT provide the emittances; results are shown in Fig. 6. The results for the vertical

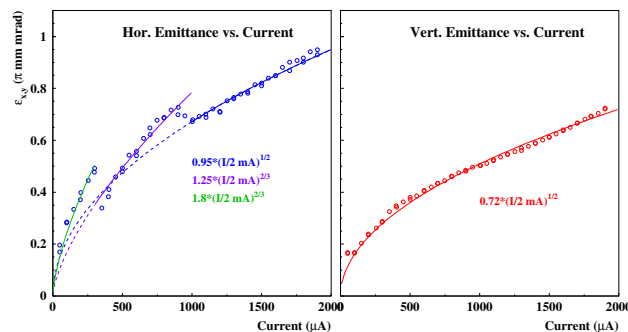


Figure 6: Emittance values as obtained from various MinT-fits (dots) of the IW2 beam profiles (production tune). The functions are not “fitted”, but just guides to the eye.

direction y are in reasonable agreement with

$$\varepsilon_y \propto \sqrt{I/I_{max}} \quad (1)$$

The transverse horizontal ε_x and the longitudinal emittance ε_z have the same behavior at high current. But at intermediate and low currents there are local variations due to the halo tails, the orientation of which changes with beam current. Depending on their orientation the halos are removed more or less effectively by the collimators. To test this interpretation, the measurements were repeated with different collimator positions. Figure 7 compares measurements with the central region collimators opened as much

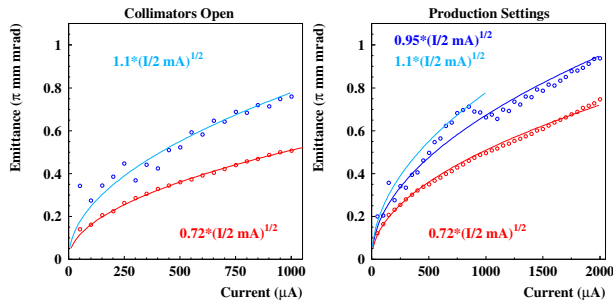


Figure 7: Left: Vertical (red dots) and horizontal (blue dots) emittance vs. beam current for collimators “open” (left) and production settings (right). The functions are guides to the eye.

as possible (at $I = 1$ mA) and compared the results with a production setup. In case of more open collimators the function $\varepsilon_{\pi \text{ mm mrad}} \approx 1.1 \sqrt{I/2 \text{ mA}}$, printed in cyan, describes the behavior up to 1 mA, while the emittance clearly reduces between 0.8 and 1 mA in case of the production settings of the collimators.

BEAM SIZE vs. CURRENT

The linear model for the core bunch in the presence of the Vortex effect gives the following relation between beam size σ , emittance ε and current I [5]:

$$\sigma^4 - \frac{4K_3 R^2}{3\gamma} \sigma - \frac{4\varepsilon^2 R^2}{\gamma^2} = 0 \quad (2)$$

where $K_3 = \frac{3qI\lambda}{20\sqrt{5}\pi\epsilon_0 mc^3 \beta^2 \gamma^3}$. If the current $I \propto \varepsilon^2$, then one obtains

$$\sigma^4 - A\varepsilon^2\sigma - B\varepsilon^2 = 0 \quad (3)$$

with two constants A and B and therefore

$$\varepsilon = \frac{\sigma^2}{\sqrt{A\sigma + B}} \quad (4)$$

and

$$I \propto \varepsilon^2 = \frac{\sigma^4}{A\sigma + B}. \quad (5)$$

Hence, for low currents ($A \ll B/\sigma$), the current will behave like $\sigma \propto I^{1/4}$ and for high currents ($A\sigma \gg B$), a proportionality $\sigma \propto I^{1/3}$. Figures 8 and 9 show profile traces of the extraction probe RIE2, Fig. 10 shows the width of the last peak when fitted by a Gaussian function. The data are in good agreement with $\sigma \propto I^{1/3}$.

OUTLOOK AND CONCLUSION

PIC-simulations of Injector II and the IW2-beamline have been done before [10, 13]. But PIC-simulations are not required to obtain the envelopes, if it is known, as in case of Injector II, that the beam is matched. The linear matching model of MinT provides sufficient information to compute the starting conditions for the calculation of the second moments of the IW2-profiles.

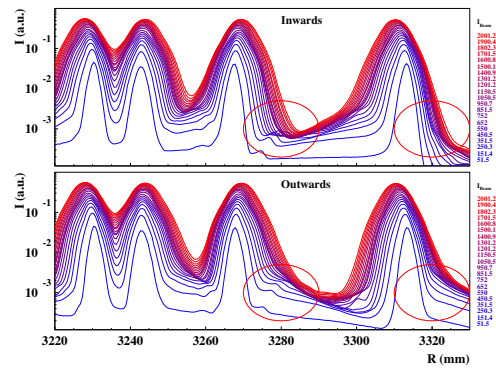


Figure 8: Scans (inward and outward) of Extraction Probe “RIE2” of Injector II in production setup. The expected location of halo traces are marked by red ellipses.

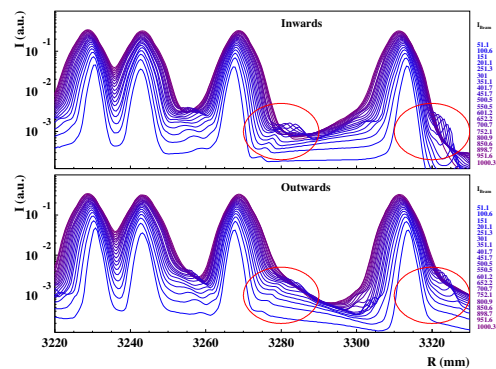


Figure 9: Same kind of scans (inward and outward) as in Fig. 8, but with “open” collimators.

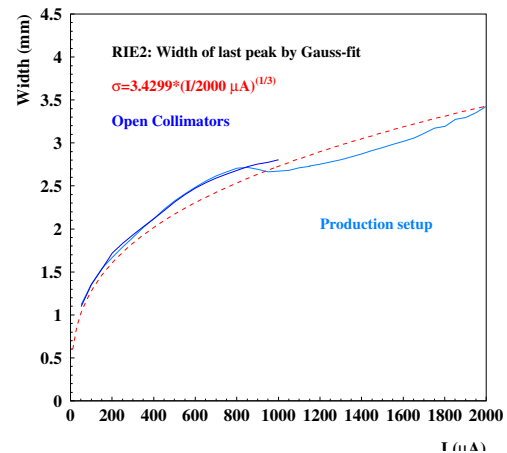


Figure 10: Transverse horizontal beam size vs. current as measured with RIE2 (Figs. 8 and 9).

The current dependence and the measured losses indicate that the beam halo is effectively removed at production current, though parts of the beam halo seem to survive up to extraction at intermediate currents.

The results are an important step towards a more detailed and comprehensive understanding of the bunch formation in Injector II.

REFERENCES

- [1] J. Grillenberger, C. Baumgarten, and M. Seidel, “The High Intensity Proton Accelerator Facility,” *SciPost Phys. Proc.*, vol. 5, no. 2, 2021.
doi:10.21468/SciPostPhysProc.5.002
- [2] M. M. Gordon, “The longitudinal space charge effect and energy resolution,” in *Proc. 5th Int. Conf on Cyclotrons and their Applications*, Oxford, UK (AERE Harwell), 1969, pp. 305–317.
- [3] C. E. Nielsen, A. Sessler, and K. Symon, “Longitudinal instabilities in intense relativistic beams,” in *Proc. 2nd Int. Conf. on High-Energy Accelerators and Instrumentation (HEACC’59)*, CERN, Geneva, Switzerland, 1959, pp. 239–252.
- [4] P. Bertrand and C. Ricaud, “Specific cyclotron correlations under space charge effects in the case of a spherical beam,” in *Proc. 16th Int. Conf. on Cyclotrons and their Applications*, East Lansing, MI, USA (MSU/NSCL), 2001, pp. 379–382.
- [5] C. Baumgarten, “Transverse-longitudinal coupling by space charge in cyclotrons,” *Phys. Rev. Spec. Top. Accel. Beams*, vol. 14, p. 114 201, 2011.
doi:10.1103/PhysRevSTAB.14.114201
- [6] R. Koscielniak and S. Adam, “Simulation of space-charge dominated beam dynamics in an isochronous avf cyclotron,” in *Proc. 1993 Particle Accelerator Conf. (PAC’93)*, Washington D.C., USA, 1993, pp. 3639–3641.
- [7] S. Adam, “Space charge effect in cyclotrons - from simulations to insights,” in *Proc. 14th Int. Conf. on Cyclotrons and their Applications*, Cape Town, South Africa, 1995, pp. 446–448. <http://accelconf.web.cern.ch/AccelConf/c95/papers/h-03.pdf>
- [8] C. Baumgarten, “Transverse-longitudinal coupling by space charge in cyclotrons,” in *Proc. 20th Int. Conf. on Cyclotrons and their Applications*, Vancouver, BC, Canada, 2013, pp. 316–319. <http://accelconf.web.cern.ch/AccelConf/CYCLOTRONS2013/papers/we2pb03.pdf>
- [9] A. Adelman *et al.*, “OPAL a versatile tool for charged particle accelerator simulations,” *arxiv:1905.06654*, 2019.
- [10] Y. J. Bi *et al.*, “Towards quantitative simulations of high power proton cyclotrons,” *Phys. Rev. Spec. Top. Accel. Beams*, vol. 14, p. 054 402, 5 2011.
doi:10.1103/PhysRevSTAB.14.054402
- [11] C. Baumgarten, “MinT: A fast lightweight envelope/monte-carlo beam optics code for the proton beamlines of the Paul Scherrer Institute,” *arXiv.org:2202.07245*, 2022.
- [12] C. Baumgarten, “A geometrical method of decoupling,” *Phys. Rev. Spec. Top. Accel. Beams*, vol. 15, p. 124 001, 2012.
doi:10.1103/PhysRevSTAB.15.124001
- [13] A. Kolano, A. Adelman, R. Barlow, and C. Baumgarten, “Intensity limits of the PSI Injector II cyclotron,” *Nucl. Instrum. Methods Phys. Res., Sect. A*, vol. 885, pp. 54–59, 2018.
doi:10.1016/j.nima.2017.12.045